Pergamon

Cement and Concrete Research 31 (2001) 905–911

CEMENT AND CONCRETE RESEARCH

# Activity of silica fume and dealuminated kaolin at different temperatures

N.Y. Mostafa[a], S.A.S. El-Hemaly[b], E.I. Al-Wakeel[c], S.A. El-Korashy[c], P.W. Brown[a,*]

[a]*136, Materials Research Laboratory, Pennsylvania State University, University Park, PA 16802, USA*
[b]*National Research Center, Cairo, Egypt*
[c]*Faculty of Science, Suez Canal University, Ismailia, Egypt*

Received 27 July 2000; accepted 22 February 2001

**Abstract**

Silica fume (SF) and dealuminated kaolin (DK) were investigated for their pozzolanic activities. The kinetics of the SF–lime and DK–lime reactions were investigated in pastes at room temperature, 100°C, and 180°C by the determination of unreacted lime and combined water. The hydration products were identified by X-ray diffraction (XRD). The variations in mechanical properties were correlated with the reaction kinetics and the hydration products formed. DK exhibited higher reactivity than SF at all temperatures studied. Tobermorite was formed at 100°C in the high-lime DK mix at 14 days and extensively formed by autoclaving at 180°C curing due to the presence of Al and sulfate in the DK. The very low C/S ratios of SF mixes and low-lime DK mix prevent tobermorite formation and promote the formation of poorly crystalline C-S-H with a higher surface area. 

*Keywords:* Silica fume; Dealuminated kaolin; Pozzolanic activity; Tobermorite; Hydrothermal

## 1. Introduction

There is currently great interest in exploiting the pozzolanic and cementitious properties of various waste materials by incorporating them in building products [1–3]. Worldwide expansion in the production and usage of autoclaved building materials has created the opportunity for replacing sand and lime (partly or wholly) by industrial by-products. These by-products may be unreactive at ordinary temperatures, but possess cementing properties at higher temperatures [4–7]. However, the utilization of by-products in autoclaved building materials is controlled by the suitability of these materials for this purpose, by the local economy and by the competitive position of other building materials within the area. Further, it may be desirable to replace sand or lime with by-products if this improves the end products or reduces the production cost through a reduction in the autoclaving time or temperature.

In a previous study [8], a comparison study was made between the reactivities of silica fume (SF) and dealuminated kaolin (DK). It was found that DK has a higher surface area (90.5 $m^2/g$) and a much higher reactivity than SF (18.8 $m^2/g$) especially during early age of hydration. The higher reactivity of DK was accounted for in part by the presence of hydrated silica (silanol groups; Si–OH).

The aim of this research is to establish optimal methods by which waste by-products can be recycled in building materials by normal curing or by reaction at higher temperatures. The pozzolanic reaction occurs mainly with lime in concrete during normal curing [9,10] or in other building materials produced at higher temperatures [5,11,12]. Establishing the mechanism of the pozzolan–lime reaction, together with determination of the mechanical properties, is fundamental for facilitating utilization and improving the characteristics of these pozzolanic materials.

## 2. Materials and methods

SF was obtained from Ferrosilicon Co., Edfo, Egypt. DK was obtained from Egyption Shaba, Egypt. It is produced as a waste by-product of aluminum extraction from calcined kaolin by sulfuric acid. The details of characterization of SF and DK are given in another paper [8].

* Corresponding author. Tel.: +1-814-865-5352; fax: +1-814-863-7040.
*E-mail address*: etx@psu.edu (P.W. Brown).

0008-8846/01/$ – see front matter 
PII: S0008-8846(01)00489-6

Table 1
Pozzolan–lime mixes

| Mix | SF | DK | $Ca(OH)_2$ | W/S |
|---|---|---|---|---|
| SFI | 80 | – | 20 | 0.70 |
| SFII | 60 | – | 40 | 0.57 |
| DKI | – | 80 | 20 | 0.40 |
| DKII | – | 60 | 40 | 0.40 |

Different mixes of these pozzolanic by-products and hydrated lime were prepared by mixing appropriate proportions of the starting materials in a ball mill for 1 h. The pastes were prepared with different water/solid ratios to attain a suitable workability as shown in Table 1. Cylindrical specimens were molded into a stainless steel mould by hand to produce specimens 2 cm in diameter and about 2 cm high. These were cured at 100% relative humidity for 12 h to attain initial setting, then cured under water at different temperatures. Specimens were cured at room temperature for 1, 3, 7, 28 and 90 days, at 100°C for 0.5, 1, 3, 7 and 14 days and at 180°C for 0.5, 2, 6, 12 and 24 h.

Compressive strengths were determined on wet samples cured at room temperature and 100°C at each time. The apparent porosities were determined using the standard liquid volume method adopted by the ASTM [13]. Prior to analyzing the phases present, the hydration reaction was stopped by immersing about 10 g of the ground specimen in about 100 ml of methanol/acetone mixture (1:1) by volume and stirring magnetically for 30 min. The solids were filtered off, washed with methanol, then dried at 105°C for 24 h. Samples cured at 180°C were tested for compressive strengths after drying at 105°C for 24 h. A specimen from each core was taken for completing other analyses. The dried samples were tested for their free lime contents using the modified Franke method [14], tested for combined water contents and examined by X-ray diffraction (XRD). The combined water contents were calculated from the loss on ignition at 900°C after correction for the loss in weight due to free lime. XRD analyses were performed using an automated diffractometer (Scintag, Sunnyvale, CA), at a step size of 0.02°, scan rate of 2° per min, and a scan range from 4° to 60° 2θ.

## 3. Pozzolan–lime reactions at room temperature

Fig. 1 shows the changes in the compressive strengths of the SF–lime and DK–lime mixes hydrated for up to 90 days. The compressive strengths increase with increasing hydration time for both pozzolan–lime mixes. SF mixes with high-lime contents (SFII) show higher compressive strength values than those with low-lime contents (SFI), at all ages of hydration. This is due both to the larger the amount of C-S-H formed and to the decrease in porosity as the W/S ratio decreases from 0.7 to 0.57 (Table 2).

DK mixes show higher compressive strength values than SF mixes, especially at early ages. However, the high-lime

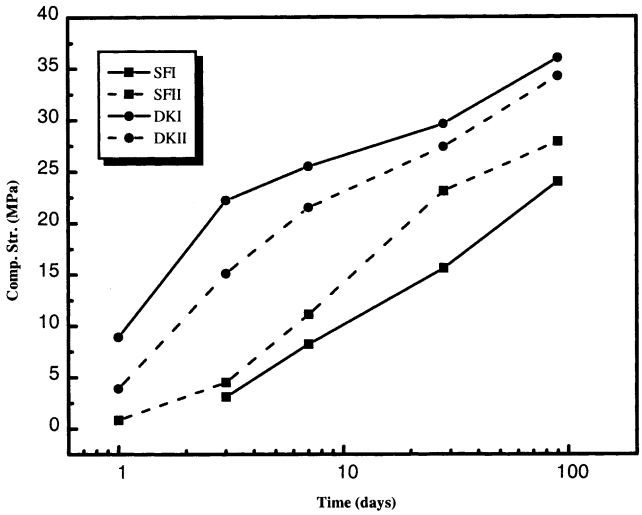


Fig. 1. Compressive strengths of SF–lime and DK–lime mixes cured at room temperature.

mix (DKII) shows lower compressive strength values than the low-lime mix (DKI). This is due to its higher initial porosity, despite of the same W/S ratio for both mixes, see Tables 2 and 3.

The kinetics of hydration were studied by determining the chemically combined water contents (Wn) and free lime contents at different ages of hydration. The results of free lime determination are given in Fig. 2. The free lime contents of all mixes decrease sharply during the first day of hydration. Beyond the first day the free lime contents for the low-lime mixes (SFI and DKI) decrease slowly. The free lime contents of the high-lime mixes (SFII and DKII) continue to sharply decrease up for the first week. This indicates that the rates of lime consumption depends on the unreacted lime contents on the mixes. DK have a higher lime fixation ability than SF at early ages, but both mixes have fixed all the lime by 90 days of hydration.

Combined water contents (Wn), as shown in Table 2, increase for both low-lime mixes (SFI and DKI) during the first 3 days, then decrease during the later ages of hydration. Mix SFII shows the same trend but with a maximum

Table 2
Combined water contents and porosity of SF and DK mixes cured at room temperature

| Mix | 1 day | 3 days | 7 days | 28 days | 90 days |
|---|---|---|---|---|---|
| *Combined water* | | | | | |
| SFI | 7.8 | 13.9 | 10.2 | 9.8 | 8.6 |
| SFII | 10.5 | 13.2 | 15.1 | 13.4 | 12.8 |
| DKI | 12.2 | 13.6 | 11.2 | 10.0 | 8.8 |
| DKII | 11.4 | 11.9 | 11.9 | 12.6 | 15.3 |
| *Porosity (vol.%)* | | | | | |
| SFI | 59 | 60 | 61 | 61 | 60 |
| SFII | 58 | 59 | 60 | 60 | 57 |
| DKI | 51 | 54 | 54 | 54 | 52 |
| DKII | 53 | 58 | 58 | 58 | 56 |

Table 3
Combined water contents and porosity of SF and DK mixes cured at 100°C

| Mix | 0.5 day | 1 day | 3 days | 7 days | 14 days |
|---|---|---|---|---|---|
| *Combined water* | | | | | |
| SFI | 10.2 | 10.6 | 10.8 | 11.1 | 8.9 |
| SFII | 13.2 | 14.1 | 14.3 | 17.8 | 13.7 |
| DKI | 11.2 | 10.9 | 12.0 | 13.8 | 12.9 |
| DKII | 12.1 | 16.1 | 16.6 | 14.3 | 13.1 |
| *Porosity (vol.%)* | | | | | |
| SFI | 60 | 59 | 60 | 60 | 59 |
| SFII | 58 | 58 | 57 | 56 | 58 |
| DKI | 50 | 51 | 53 | 53 | 52 |
| DKII | 53 | 54 | 55 | 55 | 57 |

increase in combined water content after 1 week. The combined water contents of the DKII mix show continuous slow increases after the first day of hydration.

XRD analyses were carried out on samples hydrated for 3 and 90 days. Fig. 3 shows XRD analyses for the SF mixes. The main phase detected is C-S-H. The amorphous hump associated with the SF (centered at $2\Theta = 22°$) is reduced with the progress of hydration and the peak, characteristic of C-S-H ($2\Theta = 28°$) increases. As expected, the SF broad band is still clearly detected at 28 days in the low-lime mix, indicating a large amount of SF is still unreacted.

XRD patterns of the DK mixes shown in Fig. 4 confirm the higher reactivity of DK. The low-lime mix (DKI) shows no calcium hydroxide peaks after hydration for 3 days and the peaks characteristic of $CaSO_4 \cdot 1/2H_2O$ are present. Because the small amount of C-S-H formed, cannot accommodate all the sulfate ions [15–18], $CaSO_4 \cdot 2H_2O$ was retained and converted to $CaSO_4 \cdot 1/2H_2O$ by drying at 105°C.

## 4. Pozzolan–lime reaction at 100°C

The changes in the compressive strengths of the mixes during 14 days are given in Fig. 5. The large gains in the compressive strengths occur during the first 12 h as a result of the acceleration of the lime–silica reaction at 100°C. Between 1 and 14 days, the strengths increase at a slower rate.

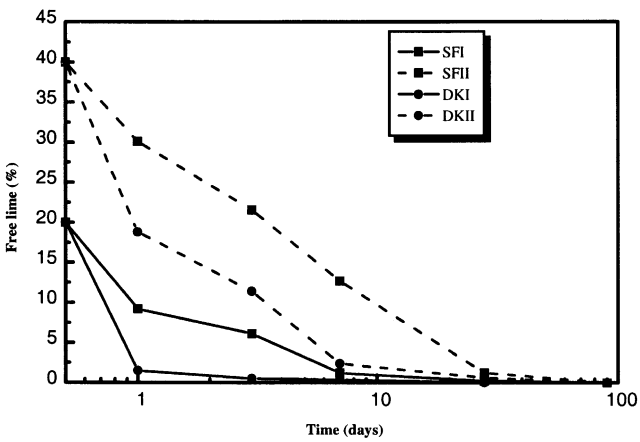


Fig. 2. Free lime contents of SF–lime and DK–lime mixes cured at room temperature.

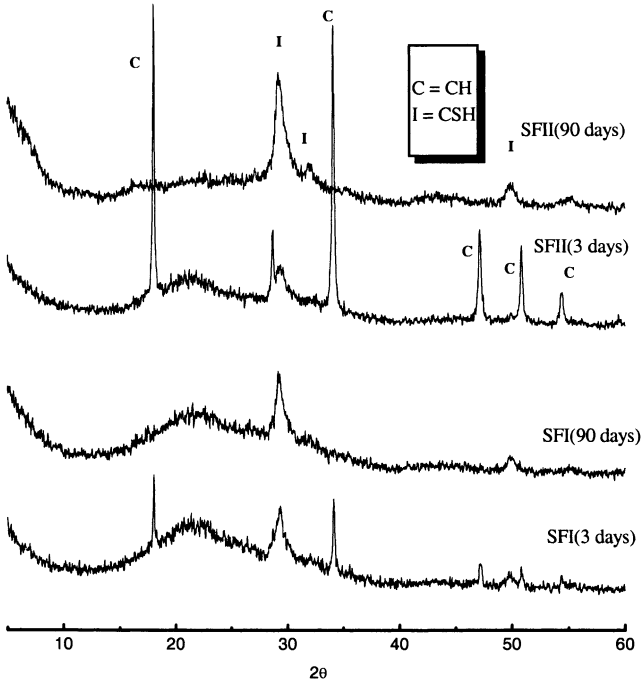


Fig. 3. XRD of SF–lime mixes cured at room temperature for different times.

The high-lime SF mix (SFII) shows larger compressive strength values than the low-lime mix (SFI) at all ages, and the strength differences are greater than those for mixes cured at room temperature. During the first 3 days, the strength of mix DKI is higher than that of mix DKII. This is due to the decrease in porosity of the initial mix and the partial transformation of the initially formed high-lime C-S-H to a C-S-H with a lower lime content and a higher binding ability [19,20]. However, between 7 and 14 days, the strength of mix DKII becomes higher due to the higher the amount of C-S-H formed.

The kinetics of hydration of the mixes were studied by determining the chemically combined water contents (Wn) and free lime contents. Fig. 6 shows the free lime contents of all mixes decrease sharply during the first 12 h of hydration. Subsequent to this, there are further decreases in free lime at slow rates. Free lime contents of DK mixes are lower than those of the corresponding SF mixes at all ages of hydration.

Combined water contents (Wn) (Table 3) typically show a large increase in the first 12 h of curing, for both mixes, followed by a continuous increase for up to 7 days curing. The exception is mix DKII, whose combined water starts to decrease after 3 days. By 14 days the combined water contents decline for all mixes. Mixes SFII and DKII show larger combined water contents at all curing times than mixes SFI and DKI.

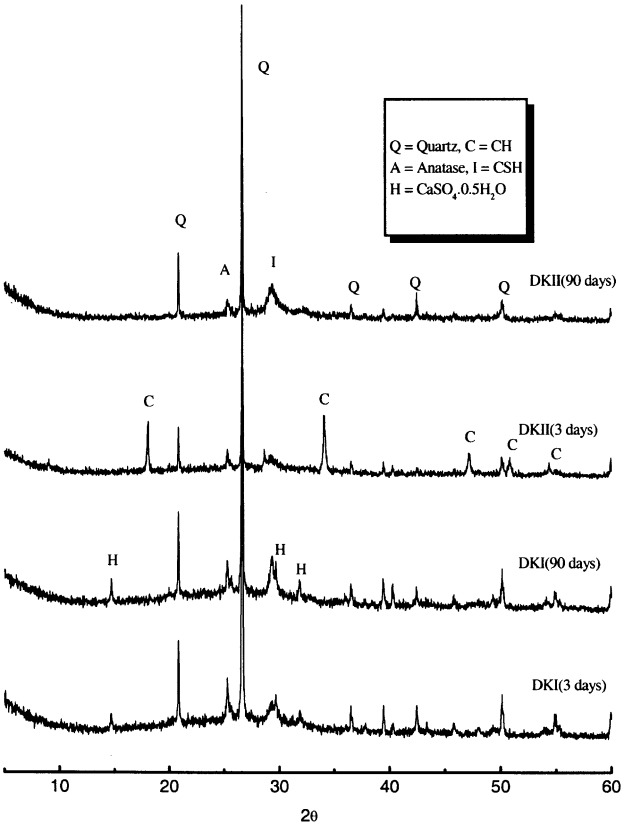


Fig. 4. XRD of DK–lime mixes cured at room temperature for different times.

XRD analyses were carried out for samples cured up to 14 days to identify the crystalline solid phases. The diffraction patterns are given in Fig. 7, indicating the main phase to be C-S-H. At room temperature, peaks characteristic of $CaSO_4 \cdot 1/2H_2O$ appeared in the low lime mix (DKI). Mix DKII shows the appearance of the peaks of tobermorite, but no hemihydrate peaks appear. This indicates that tobermorite can be formed at 100°C in the presence of aluminum and

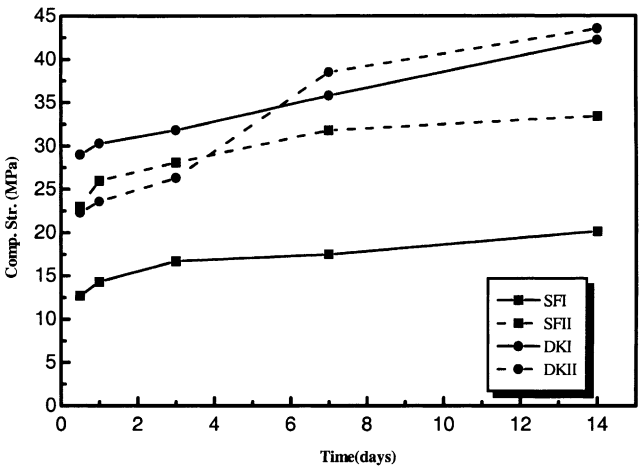


Fig. 5. Compressive strengths of SF–lime and DK–lime mixes cured at 100°C.

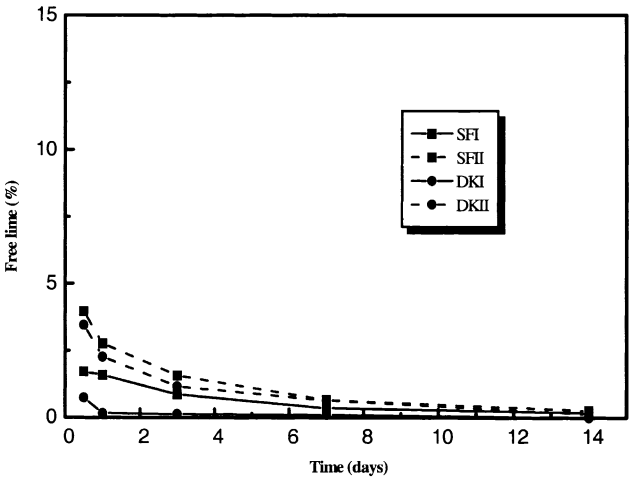


Fig. 6. Free lime contents of SF–lime and DK–lime mixes cured at 100°C.

sulfate ions by using very reactive silica. Sauman [21] and others [22] found that sulfate ions substitute in the lattice of 11 Å tobermorite at 180°C and accelerate its formation from C-S-H gel and that aluminate ions condition the effect of

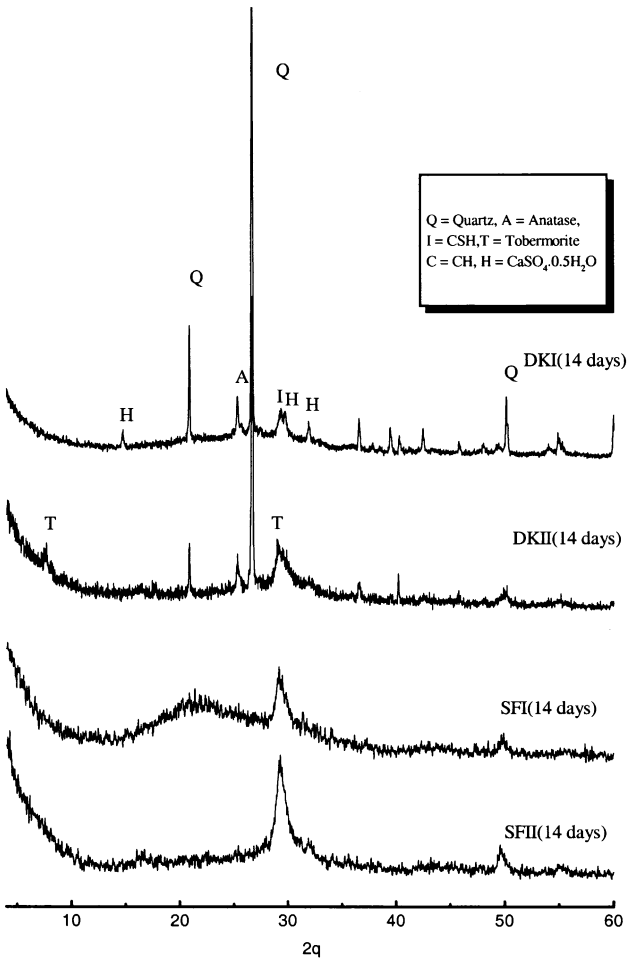


Fig. 7. XRD of SF–lime and DK–lime mixes cured at 100°C for different times.

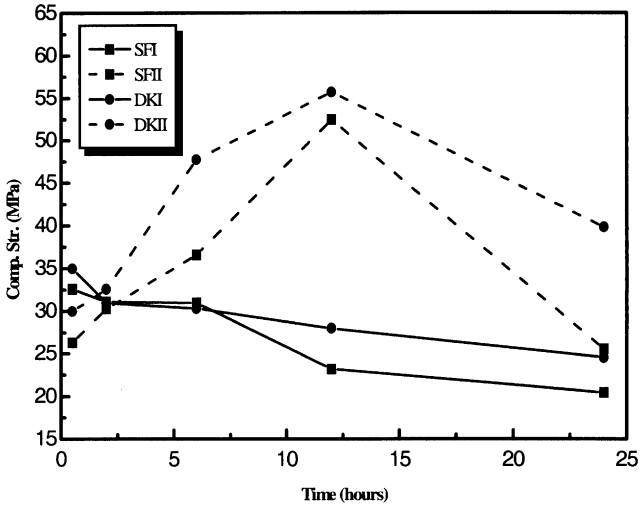


Fig. 8. Compressive strengths of SF–lime and DK–lime mixes cured at 180°C.

sulfate. The presence of quartz in DK may also accelerate tobermorite formation. Chan and Mitsuda [23] found that when colloidal silica was the sole silica source with CaO, C-S-H did not convert to tobermorite even after 20 h autoclaving at 180°C. However, samples made with quartz and colloidal silica did convert to tobermorite.

## 5. Pozzolan–lime reaction at 180°C

The changes in the compressive strengths of the pozzolan–lime mixes autoclaved at 180°C are given in Fig. 8. At this temperature, mix SFI (20% lime) shows higher compressive strengths than mix SFII (40% lime) at curing times of 0.5 and 2 h. Because, free lime is nearly consumed after autoclaving for 0.5 h, the initially formed high-lime C-S-H appears to react with silica and transform to a low-lime C-S-H having a higher binding ability.

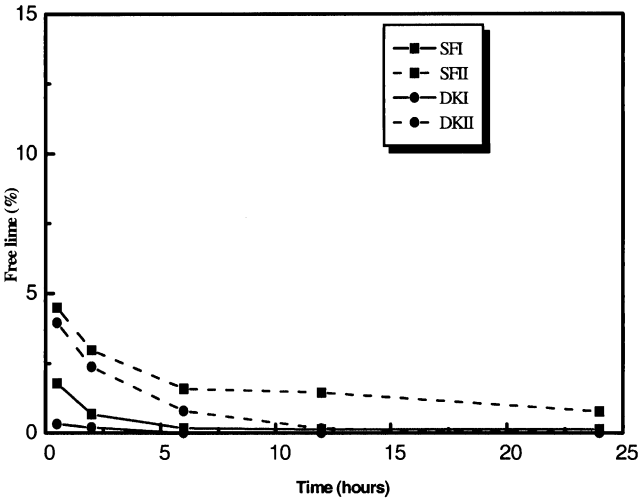


Fig. 9. Free lime contents of SF–lime and DK–lime mixes cured at 180°C.

Table 4
Combined water contents and porosity of SF and DK mixes cured at 180°C

| Mix | 0.5 h | 2 h | 6 h | 12 h | 24 h |
|---|---|---|---|---|---|
| *Combined water* | | | | | |
| SFI | 10.6 | 11.6 | 12.0 | 11.9 | 10.8 |
| SFII | 13.3 | 16.4 | 16.4 | 14.3 | 20.6 |
| DKI | 14.5 | 16.1 | 14.6 | 14.2 | 14.9 |
| DKII | 13.2 | 15.0 | 14.4 | 14.3 | 16.7 |
| *Porosity (vol.%)* | | | | | |
| SFI | 59 | 59 | 59 | 58 | 58 |
| SFII | 57 | 57 | 56 | 56 | 58 |
| DKI | 49 | 51 | 52 | 51 | 51 |
| DKII | 50 | 51 | 54 | 55 | 54 |

Mix SFI and mix DKI show continuous declines in compressive strength with increased curing time due to the transformation of the initially formed amorphous, high surface area C-S-H to C-S-H with a lower surface area [24], thereby lowering the binding ability. The strengths of mixes SFII and DKII markedly increase with autoclaving time up to 12 h, before decreasing.

The results of the free lime determination are given in Fig. 9. The free lime contents of all mixes decrease sharply during the first 2 h of autoclaving. Further autoclaving results in decreases in free lime contents at slow rates. Combined water contents (Wn) (Table 4) also show large increases with a curing time of 2 h. Mix SFI reached a maximum Wn after 6 h autoclaving time, then the Wn smoothly decreased with further curing. Mix SFII show higher combined water contents at all curing times but it also started to decline after 12 h of autoclaving.

XRD analyses were carried out on samples cured for 6 and 24 h. The diffraction patterns are given in Figs. 10 and

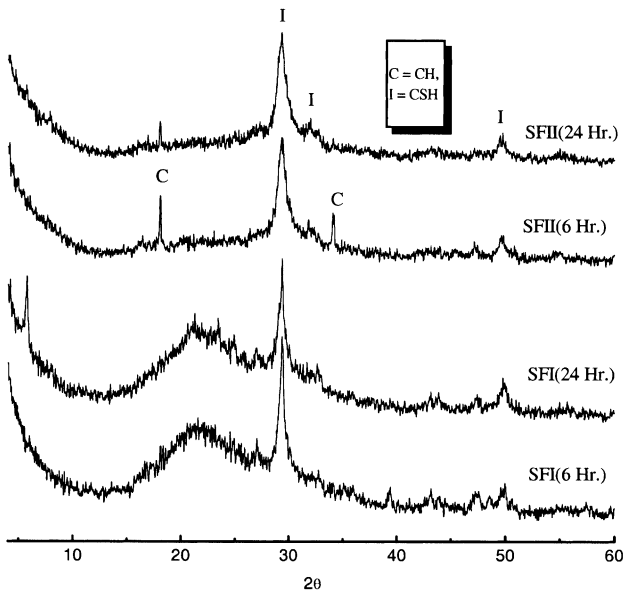


Fig. 10. XRD of SF–lime mixes autoclaved at 180°C for different times.

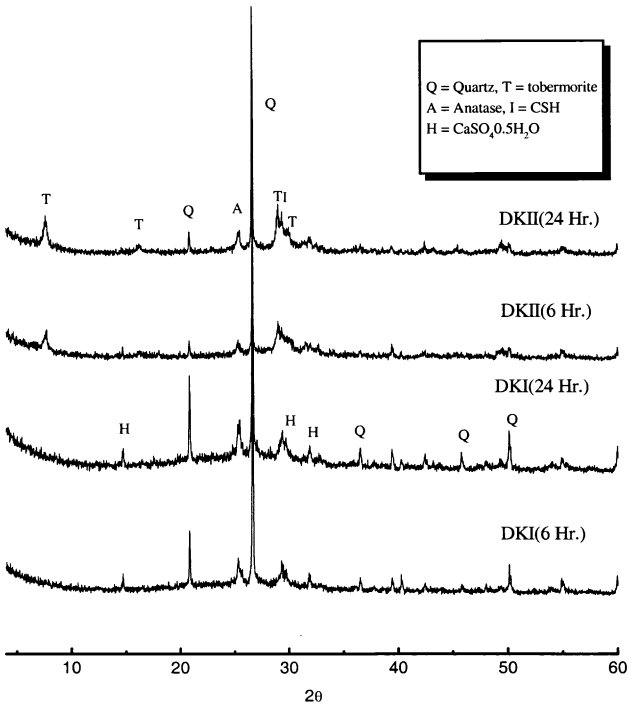


Fig. 11. XRD of DK–lime mixes cured at 180°C for different times.

11 for SF and DK mixes, respectively. XRD analyses of SF mixes indicates the main phase in high-lime mix (SFII) to be C-S-H. The mix with lower lime content (SFI) shows the presence of 14 Å tobermorite [PDF 29-0331] peaks at 24 h autoclaving. The high-lime mix DKII shows tobermorite peaks after 6 and 24 h. Low-lime mix DKI shows no tobermorite peaks, but peaks characteristic of C-S-H are present. This indicates that a low C/S ratio promotes the formation of poorly crystalline C-S-H and prevents the tobermorite formation in spite of the presence of sulfate, aluminate and quartz. The peaks characteristic of $CaSO_4 \cdot 1/2H_2O$ are again present.

## 6. Conclusions

Although DK has a lower reactive silica content (less than 75%, due to the presence of quartz) than SF (96%), its reactivity is much higher. DK mixes attained higher compressive strengths than those containing SF, especially at short hydration ages. However, both DK and SF were able to fix all the CH present. The higher reactivity of DK can be accounted for by its higher surface area (90.5 m2/g) and the presence of hydrated silica (silanol groups; $Si_s$–OH), as described in a prior study [8].

In spite of its lower surface area (18.8 $m^2/g$), SF mixes require more mixing water to obtain approximately the same workability as the DK mixes. This is due to the presence of a considerable amount of adsorbed water on the surface of DK. This adsorbed water which is strongly hydrogen bonded to silanol groups (Si–OH:$OH_2$) [25,26] prevents further adsorption of mixing water as in the case of SF.

Increasing the hydration temperature to 100°C increases the rate of hydration of both SF and DK. The hydration of the DK mixes indicate that tobermorite can be formed at 100°C in the presence of aluminum and sulfate ions by using very reactive silica, provided the C/S ratio does not decrease below certain limits. This is because sulfate ions substitute the lattice of 11 Å tobermorite, and accelerates its formation from the C-S-H gel while aluminum ions condition the effect of sulfate [22,23].

Hydration at 180°C increases the compressive strengths of both pozzolan mixes. Low-lime mixes reach the optimum strength after 0.5 h, and high-lime mixes reach the optimum at 12 h. Mix DKII forms tobermorite, but C-S-H gel persists until 24 h in both SF mixes and low-lime DK mix (DKI). Because tobermorite is the principal binding phase in autoclaved building materials, there is great interest in optimizing its conversion from C-S-H. Replacing quartz, the usual silica source in autoclaved materials, with a more reactive silica (amorphous silica) increases the rate of C-S-H formation, but decreases the rate of conversion of C-S-H to tobermorite [23,27]. Okada et al. [28] noted that the C/S ratio of the initially formed C-S-H gel controls the rate of its transformation to tobermorite. In CaO and quartz mixtures (Ca/Si = 0.8), the initial C-S-H with a Ca/Si of 1.69 transformed to tobermorite having a C/S $< 0.9$. In a comparison sample made with silicic acid and CaO (C/S = 0.8), the initial C-S-H had a Ca/Si = 0.81, and tobermorite crystallization was significantly slower. Okada et al.'s results [28] were confirmed by Sato and Grutzeck [29] using $^{29}Si$ NMR to study samples prepared from CaO and quartz, silicic acid, or colloidal SF at 180°C. The C-S-H which formed initially in the quartz samples was characterized by a low Q2/Q1 ratio (i.e., short chains, dimers), and tobermorite crystallized by 4 h. In samples made from silicic acid and SF, the initial C-S-H had a high Q2/Q1 plus Q3 (i.e., long chains, some cross-linking). Even after 24 h, these samples did not convert to crystalline tobermorite. Tobermorite formed easily from the C-S-H with high C/S ratio, but not from the Si-rich ones, which indicates that the C-S-H gel structure affects the ease of tobermorite crystallization. The presence of long, cross-linked chains in the Si-rich C-S-H retards the rearrangement of silica tetrahedra that is needed to form tobermorite. On the other hand, the short chains and dimers in the Ca-rich C-S-H can rearrange more easily to form crystalline tobermorite. In the present study, the low C/S ratio promotes the formation of poorly crystalline C-S-H and prevents the tobermorite formation in spite of the presence of sulfate aluminum and quartz, which had been shown to promote tobermorite formation [21–23].

The present study has shown that DK can be used as a valuable additive to blended cement or autoclaved building materials. The addition of DK in autoclaved building materials is expected to accelerate tobermorite formation

unlike SF. This may used to reoptimize the production cost to lower autoclaving time or lower autoclaving temperature. DK can also be used in the production of low-strength lightweight building units, such as bricks at room temperature by blending with CH. The former is an economical option for developing countries.

## Acknowledgments

P.W.B. acknowledges NSF grant no. DMR 9510272.

## References

[1] ASTM C595, Standard specification for blended hydraulic cements, 1998.
[2] S. Chardra, Waste Materials used in Concrete Manufacturing, Noyes Publications, Westwood, NJ, 1997, pp. 242–243.
[3] H.F.W. Taylor, Cement Chemistry, Academic Press, New York, 1990, p. 367.
[4] G.E. Bessey, in: H.F.W. Taylor (Ed.), Chemistry of Cement vol. II, Academic Press, London, 1964, p. 107 (Chap. 16).
[5] N. Isu, K. Sasak, H. Ishida, T. Mitsuda, Mechanical properties evolution during autoclaving process of aerated concrete using slag: I. Tobermorite formation and reaction behavior of slag, J. Am. Ceram. Soc. 77 (8) (1994) 2088–2092.
[6] S. Grzeszczyk, J. Szuba, Hydration reactivity of crystalline and vitrified diopside under hydrothermal conditions, J. Am. Ceram. Soc. 73 (7) (1990) 2006–2008.
[7] N. Hara, N. Inoue, Formation of jennite from fumed silica, Cem. Concr. Res. 10 (1980) 677–682.
[8] N.Y. Mostafa, S.A.S. El-Hemaly, E.I. Al-Wakeel, S.A. El-Korashy, P.W. Brown, Characterization and evaluation the pozzolanic activity of Egyptian industrial by-products: I. Silica fume and dealuminated kaolin, Cem. Concr. Res. 31 (3) (2001) 467–474.
[9] P. Ubbriaco, F. Tasselli, A study of the hydration of lime–pozzolan binders, J. Therm. Anal. 52 (1998) 1047–1054.
[10] V. Lilkov, V. Stoitchkov, Effect of the 'Pozzolit' active mineral admixture on the properties of cement mortars and concretes: Part 2. Pozzolanic activity, Cem. Concr. Res. 26 (7) (1996) 1073–1081.
[11] B. Kurbus, F. Bakula, R. Gabrovsek, Reactivity of $SiO_2$ fume from ferrosilicon production with $Ca(OH)_2$ under hydrothermal conditions, Cem. Concr. Res. 15 (1985) 134–140.
[12] S.A.S. El-Hemaly, A.S. Taha, H. El-Didamony, Influence of slag substitution on some properties of sand–lime aerated concrete, J. Mater. Sci. 21 (1986) 1293–1296.
[13] ASTM C 373-88, Water absorption, bulk density, apparent porosity and apparent specific gravity of fired whiteware products, 1999.
[14] ASTM C114, Standard test methods for chemical analysis of hydraulic cement, 1999.
[15] G.L. Kalousek, Analyzing $SO_3$-bearing phases in hydrated cement, Mater. Res. Stand. 6 (1965) 292–304.
[16] I. Older, S. Abdul-Maula, Z. Lu, Effect of hydration temperature on cement paste structure, microstructural development during hydration of cement, L. Struble, P. Brown (Eds.), Proc. Mater. Res. Soc., Pittsburgh 85, 1987, pp. 139–144.
[17] I. Older, Interaction between gypsum and CSH-phase formed in $C_3S$ hydration, Proc. 7th Int. Congr. Chem. Cem., Paris, vol. IV, 1980, pp. 493–495.
[18] I.G. Richardson, G.W. Groves, The incorporation of minor and trace elements into calcium silicate hydrate (C-S-H) gel in hydrated cement paste, Cem. Concr. Res. 23 (1993) 131–138.
[19] H.F.W. Taylor, Proposed structure for calcium silicate hydrate gel, J. Am. Ceram. Soc. 69 (6) (1986) 464.
[20] J.M. Crennan, S.A.S. El-Hemaly, H.F.W. Taylor, Autoclaved lime-quartz materials: I. Some factors influencing strength, Cem. Concr. Res. 7 (1977) 493–502.
[21] Z. Sauman, Influence of $SO_4^{2-}$ ions on the formation of 11Å-tobermorite, 3rd Int. Symp. Auto. Calc. Silic. Chem., Brno vol. 25, 1973, 47–59.
[22] N.Y. Mostafa, Factors effecting the hydrothermal reactions in $CaO–SiO_2–H_2O$ system, MSc thesis, Suez Canal University, December 1995.
[23] C.F. Chan, T. Mitsuda, Formation of 11Å tobermorite from mixtures of lime and colloidal silica with quartz, Cem. Concr. Res. 8 (1978) 135–138.
[24] G. Gung, H. Kim, S.G. Kim, Preparation and characterization of lime–silica solids, Ind. Eng. Chem. Res. 39 (5) (2000) 1264–1270.
[25] M.A. Vincente, M. Suarez, J.D. Lopez-Gonzalez, M.A. Banares-Munoz, Characterization, surface area, and porosity analyses of the solids obtained by acid leaching of a saponite, Langmuir 12 (1996) 566–572.
[26] S. Chuang, G.E. Maciel, A detailed model of local structure and silanol hydrogen bonding of silica gel surface, J. Phys. Chem. B 101 (1997) 3052–3064.
[27] S.A.S. El-Hemaly, T. Mitsuda, H.F.W. Taylor, Synthesis of normal and anomalous tobermorite, Cem. Concr. Res. 7 (1977) 429–438.
[28] Y. Okada, M. Shimoda, T. Mitsuda, H. Toraya, Synthesis of tobermorite: NMR spectroscopy and analytical electron microscopy, Onoda Co. Rep. 42 (1990) 123 (Part 2).
[29] H. Sato, M.W. Grutzeck, Effect of starting materials on the synthesis of tobermorite, in: F.P. Glasser, G.J. McCarthy, J.F. Young, T.O. Mason, P.L. Pratt (Eds.), Advanced Cementitious Systems: Mechanisms and Properties, Proc. Mater. Res. Soc. Symp., Boston, MA, Dec., 1991, Mat. Res. Soc., Pittsburgh, PA, 1992, pp. 235–240.